Atomic resolution force microscopy imaging on a strongly ionic surface with differently functionalized tips

T. Arai[a)]
Graduate School of Natural Science and Technology, Kanazawa University, Kakuma-machi, Kanazawa, Ishikawa 920-1192, Japan

S. Gritschneder, L. Tröger, and M. Reichling[b)]
Fachbereich Physik, Universität Osnabrück, Barbarastraße 7, 49076 Osnabrück, Germany

Three types of tips for noncontact atomic force microscopy imaging, namely, a *silicon nanopillar tip*, a *carbon nanopillar tip*, and a *fluoride cluster tip*, are prepared for atomic resolution imaging on the $CaF_2(111)$ surface. The most enhanced atomic corrugation is obtained with the fluoride cluster tip prepared by gently touching the fluorite surface. Atom resolved images are much harder to obtain with the other tips. This demonstrates the importance of having a polar tip for atomic resolution imaging of an ionic surface and supports the general notion that a surface is best imaged with a tip of the same material. © *2010 American Vacuum Society.*
[DOI: 10.1116/1.3511505]

I. INTRODUCTION

Noncontact atomic force microscopy (NC-AFM) has greatly succeeded in imaging and manipulating a variety of surfaces of metals,[1,2] semimetals,[3–5] semiconductors,[6–10] and insulators.[11–14] In particular, atom-resolved imaging on terraces[15] and at step edges[16–18] on $CaF_2(111)$, which is the surface of interest for this study, is well established and understood by extensive theoretical modeling.[19,20] However, a full quantitative understanding of contrast formation in imaging and atomic precision force controlled manipulation requires the preparation of force microscopy tips with well defined shape and functionality and great efforts have been made to produce such tips.[21–24] At present, however, direct evidence and analytical methods for determining the species at the end of the probing tip are generally missing and the accumulation of indirect evidence and trial of controlling the tip apex at the atomic level are significant challenges to understanding NC-AFM imaging mechanisms. An exception to this is a recent result in force microscopy at cryogenic temperatures, where the tip can be prepared with the atomic precision known from low-temperature scanning tunneling manipulation experiments and is, therefore, known to be a specific molecule.[25] This method is, however, not generally applicable and a common method to yield quantitative imaging is a comparison of high quality atomically resolved images obtained with different tips of unknown composition to results from image calculations based on advanced computational methods[26] performed for a larger set of plausible and robust tips.[27] Recently, using this approach to explain atomic contrast formation on the $TiO_2(110)$ surface, the four most prominent NC-AFM imaging modes for this surface could be identified and explained in very detail, allowing for an immediate identification of atomic surface features on the un-

reconstructed surface[28–31] as well as on a (1×2) reconstructed surface.[32] In general, the atomic species at the tip apex should be altered depending on the investigated sample material as the atomic contrast in NC-AFM imaging strongly depends on the preferential interaction between tip and sample atoms. For imaging the $CaF_2(111)$ surface, different tip models have already been investigated by theoretical simulation and there is a detailed understanding of the characteristics of the interaction between these model tips and the fluorite surface.[33–35]

In this article, we report on the characteristics of atomic contrast formation with three different tips for imaging the strongly ionic $CaF_2(111)$ surface cleaved and measured in ultrahigh vacuum (UHV). These tips are (1) a tip having a clean silicon nanopillar grown from a heated silicon sample in the NC-AFM (*silicon nanopillar tip*),[23] (2) a tip with a carbon nanopillar deposited by electron beam irradiation in a scanning electron microscope (*carbon nanopillar tip*),[36] and (3) an as-supplied commercial Si tip covered with a native oxide layer and modified by gently touching the sample (*fluoride cluster tip*). With these tips, we measure the $CaF_2(111)$ surface under similar conditions and compare the strength of the apparent atomic contrast patterns with each other.

II. EXPERIMENTAL DETAILS

NC-AFM imaging is performed with a commercial atomic force microscope (AFM) (UHV-AFM/STM, Omicron NanoTechnologyGmbH, Taunusstein, Germany) in an ultrahigh vacuum environment maintaining a base pressure in the low 10^{-10} mbar range, which ensures that the cleaved fluorite surface remains free of adsorbates for several days. The resonance frequency f_0 of the silicon cantilevers used (type FMR, Nanoworld AG, Neuchâtel, Switzerland) is typically 70 kHz, their force constant is typically 2.8 N/m, and their effective Q-factor[37] is about 30 000 as cantilevers are coated

_____

a)Electronic mail: arai@staff.kanazawa-u.ac.jp
b)Electronic mail: reichling@uos.de

with a 30 nm aluminum layer on the detector side to increase the reflectivity for the light of the detection system. Cantilevers are excited to oscillation with an amplitude stabilized to 35 nm. The tips of the as-supplied cantilevers are covered with a layer of native silicon oxide of unknown thickness, structure, and composition. Prior to their use in imaging experiments, all cantilevers are baked at 110 °C for 50 h during bakeout of the UHV chamber. This procedure preserves the oxide layer and tip functionalization but removes water and other volatile contaminants from the tip and the cantilever. The shape of all tips before and after their modification and NC-AFM imaging is observed with a field emission scanning electron microscope (SEM) JSM-6500F (JEOL, Eching, Germany).

Samples are high quality CaF_2 single crystals (Korth Kristalle, Altenholz, Germany) cleaved along the (111) plane in the UHV chamber.[38] Surface potentials are to a large extent compensated by applying an appropriate bias voltage V_s between the tip and the metallic plate supporting the crystal at its back, so that the electrostatic force is minimized.[39] To probe contrast formation at various length scales, different scanning areas are investigated. For regions wider than 100 $\times$ 100 nm^2, NC-AFM topography images and z profiles are taken in the constant frequency shift (Δf) mode together with the damping signal. The scan speed v_t in the fast scanning direction is typically 500 nm/s for large area scans, yielding a typical image acquisition speed of 1 line/s. For regions smaller than 10×10 nm^2 that do not contain step edges, NC-AFM images of the detuning signal and Δf profiles are taken in the constant height mode with a scan speed of typically 30 nm/s to study atomic resolution contrast formation. Results presented here have been obtained with the commercial AFM instrument prior to its optimization,[40] explaining the somewhat high noise level in the images.

III. TIP PREPARATION

As-supplied oxide covered single crystal silicon tips are functionalized in three different ways, namely by (1) a *silicon nanopillar*, (2) a *carbon nanopillar* and (3) a *fluoride cluster* as visualized in the SEM micrographs compiled in Fig. 1. (1) We grow a silicon nanopillar as shown in the SEM images of Figs. 1(a) and 1(b) by dipping the tip in a Si(111) sample heated in the NC-AFM stage. To accomplish this, the silicon sample is flashed to 1250 °C for cleaning in the preparation stage, and then kept at 600 °C by direct current heating in the NC-AFM stage. The Si tip is brought to the heated sample using the AFM coarse approach mechanism. After an attractive force between the tip and the silicon sample is detected, the silicon tip is gently brought in touch with the surface using the fine positioning mechanism of the AFM until the force becomes repulsive. Afterwards, the cantilever, having picked up the nanopillar, is quickly retracted until the attractive force is in the range of 20–50 nN. This force is due to meniscus formation of a Si bridge between the tip and the sample at the contact point. Thereafter, the tip is slowly retracted, resulting in a slowly decreasing attractive force, and at last breaking the Si bridge. Consequently, a
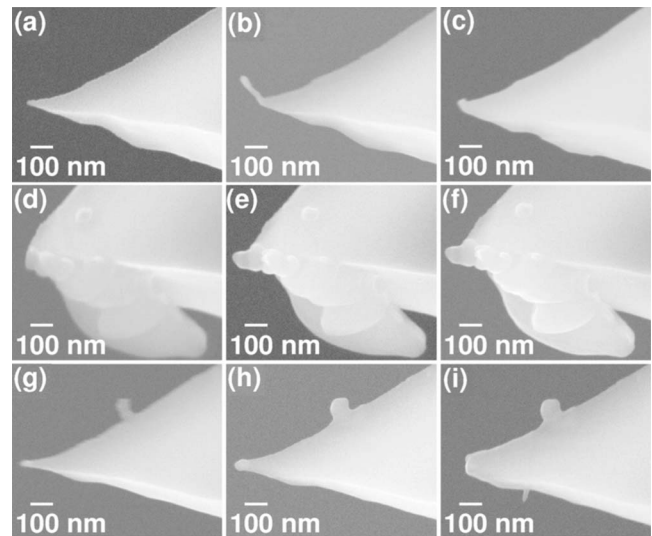

FIG. 1. SEM micrographs of force microscopy tips used for the present studies. [(a)–(c)] Silicon nanopillar tip. (a) As-supplied oxidized silicon tip. (b) The same tip after producing a silicon pillar at its end by dipping the tip into a hot silicon surface. (c) The same tip after a hard crash onto the surface. [(d)–(f)] Carbon nanopillar tip. (d) As-supplied oxidized silicon tip with contamination on lower side. (e) Carbon nanotip grown by high intensity electron irradiation in the hydrocarbon containing residual gas of the SEM. (f) The same tip after a hard crash onto the surface. [(g)–(i)] Fluoride cluster tip. (g) As-supplied oxidized silicon tip with contamination on upper side. (h) The same tip after gently touching the surface to pick up a substrate cluster. (i) The same tip after a hard crash onto the surface.

silicon nanopillar extracted from the Si crystal is grown at the Si tip apex. We anticipate that the nanopillar is a clean single crystal.[23] Although a long Si nanopillar can be grown as demonstrated in Fig. 1(b), a shorter silicon nanopillar is normally used for NC-AFM imaging as the nanopillar is easily broken by crashing it into the sample surface as shown in Fig. 1(c). A tip prepared by this procedure is further on denoted as a silicon nanopillar tip. (2) Figures 1(d) and 1(e) demonstrate another way of tip functionalization. The respective SEM micrographs show a tip before and after the deposition of a carbon nanopillar by scanning the tightly focused SEM electron beam of 8 keV electrons at the maximum magnification around the tip apex. By this procedure, which is based on the decomposition of hydrocarbons from the residual gas in the SEM chamber,[36] we grow carbon tips with a length of about 100 nm. It should be noted that the carbon tip is robust against crashing into the surface. Figure 1(f) shows the tip after being strongly crashed into the sample surface; however, no apparent change is observed and we anticipate that the deposited carbon tip is as hard as diamondlike carbon.[36] A tip prepared after this recipe is further on called a carbon nanopillar tip. (3) The last preparation procedure is an *in situ* functionalization during imaging by picking up material from the investigated surface. Figure 1(g) shows the SEM micrograph of an as-supplied tip. Immediately after the SEM observation of the tip, we introduce the tip into the NC-AFM chamber and bake it as described above. While scanning the CaF_2(111) surface for NC-AFM imaging, we invoke a very gentle contact between the tip and
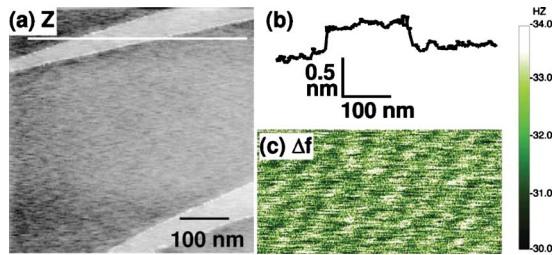
FIG. 2. (Color online) NC-AFM images of the $CaF_2(111)$ surface obtained with the silicon nanopillar tip: $f_0=71.5$ kHz and $V_s=2.6$ V. (a) Large area topography image: $\Delta f=-6.0$ Hz and $v_t=500$ nm/s. (b) Cross section along the line shown in (a). (c) High resolution detuning image revealing faint atomic contrast. Frame size 1.4×2.8 nm^2 and $v_t=30$ nm/s.

FIG. 3. (Color online) NC-AFM images of the $CaF_2(111)$ surface obtained with the carbon nanopillar tip: $f_0=71.0$ kHz and $V_s=1.0$ V. (a) Large area topography image: $\Delta f=-12.2$ Hz and $v_t=1000$ nm/s. (b) Cross section along the line shown in (a). (c) High resolution detuning image revealing faint atomic contrast. Frame size 1.4×2.8 nm^2 and $v_t=30$ nm/s.

the surface. Subsequent SEM imaging of the tip after having finished measurements and removing the tip from the NC-AFM chamber [Fig. 1(h)] reveals no apparent change in shape. After SEM observation, the tip is introduced again into the NC-AFM chamber and intentionally crashed harder onto the sample surface. Figure 1(i) shows a SEM image of the crashed tip, revealing that the tip apex of about 100 nm was blown off. It is worth noting that the difference between gently touching the surface and a tip crash can often be detected as a change in the damping signal of the NC-AFM imaging. For example, during free oscillation far away from the sample, the damping signal typically amounts to 0.9 V and increases to 1.5 V after touching the surface. As a reference, for imaging the surface with atomic resolution, the damping signal is at a level of typically 1.2 V. On the other hand, the signal increases instantaneously to a value above 5 V after a tip crash. Hence, the tip functionalization by touching the surface is a controlled process for the production of a polar tip made from the sample material. A tip that has gently touched the CaF_2 sample and picked up a nanoscopic material cluster is further on referred to as a fluoride cluster tip.

IV. NC-AFM CONTRAST FORMATION

We use these three functionalized tips for the NC-AFM imaging of $CaF_2(111)$. Generally, the cleaved $CaF_2(111)$ surface exhibits atomically flat terraces with a few steps in a square of several hundred nanometer side length. The apparent step profile reflects the tip shape and electric charge present on the tip and at the step edge.[41] We start the investigation for each tip with large scale topographic imaging and then decrease the imaging area to one terrace switching from the topography to the constant height mode for atomic resolution imaging. Immediately after the preparation of the silicon nanopillar tip, it is applied to imaging the $CaF_2(111)$ surface; the respective topographic NC-AFM data are shown in Fig. 2(a) with the profile extracted shown in Fig. 2(b). The steps appear to be regular, although they partially appear bright. In a damping image simultaneously recorded with Fig. 2(a) (not shown), no bright featured lines appear at the steps. This indicates that the tip is not charged as damping images obtained with a charged tip exhibit bright lines over the steps, as it is partly found in the damping image of Fig.
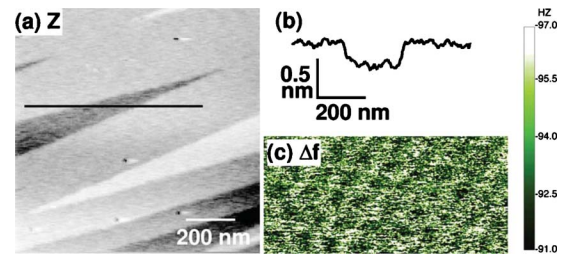
4(b), which will be discussed later. Upon a closer approach on a terrace, we observe a faint atomic corrugation, as shown in Fig. 2(c). The apparent atomic contrast is about 1.5 Hz and close to the detection limit. A clean tip is known to be appropriate for imaging silicon surfaces because of the strong chemical interaction between the Si atoms at the tip apex and silicon atoms on the surface[8,42] and has also been proposed to yield a good chemical contrast on $CaF_2(111)$.[34] It has, however, also been pointed out that a silicon based tip generally exhibits a considerably smaller interaction with the ionic surface than a polar tip.[35] Apparently, for the clean silicon tip that we anticipate to be active in this experiment, the interaction is so weak that detailed contrast features are hidden below the noise floor.

Figure 3(a) shows the NC-AFM topography result obtained for a carbon nanopillar tip. The profile along the line indicated in Fig. 3(a) is shown in Fig. 3(b). No apparent change is observed by SEM even after crashing the tip into the sample, as shown in Fig. 1(f), which can be attributed to its hardness. Only weak atomic corrugation is found with the carbon nanopillar tip, as shown in Fig. 3(c), where the atomic corrugation is roughly 2 Hz. Therefore, a carbon tip is also not very suitable for atomic resolution imaging on $CaF_2(111)$. There is no calculation of the interaction between a carbon tip and an ionic surface available; however, we understand that the nonpolar carbon tip, which can be expected to be more susceptible to covalent rather than ionic bonding, does not yield a large atomic scale contrast. However, from a more general viewpoint of tip selection, a carbon tip has the advantage of a long lifetime and a sharp tip end. Therefore, it may be a good choice for atomic scale imaging, for instance, of molecular layers on surfaces.

The as-supplied tip is covered with native oxide and may carry charge. Therefore, it often exhibits a fluctuating behavior at the beginning of imaging, but after several imaging cycles, the charge is mostly removed from the tip, resulting in more stable imaging conditions. Figure 4(a) shows an image taken with an as-supplied tip after several preceding imaging cycles. The tip is scanned from left-bottom to top-right. The beginning of topography shows the usual cut profile without any extraordinary jumps at the steps. However, in the uppermost part of the image where the tip is brought closer to the surface and touches the sample of CaF_2
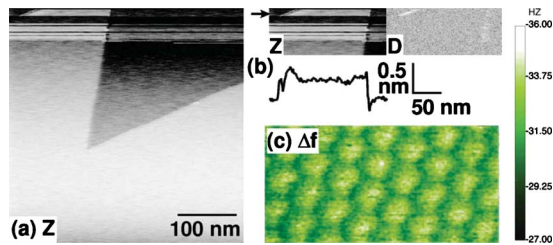
FIG. 4. (Color online) NC-AFM images of the $CaF_2(111)$ surface obtained with the as-supplied tip that is converted into a fluoride cluster tip: f_0=77.0 kHz and V_s=1.8 V. (a) Large area topography image: Δf= −3.5 Hz and v_t=500 nm/s. (b) Detail of topography (Z) and simultaneously recorded dissipation (D) signals and cross section along the line shown in (a). The arrow indicates the final tip change resulting in the formation of the fluoride cluster at the tip end. (c) High resolution detuning image revealing strong atomic contrast. Frame size 1.4×2.8 nm^2 and v_t =30 nm/s.

gently at step edges, clusters of the sample are most probably transferred from the surface to the tip apex. During such tip changes, the image appears to be unstable for a while but recovers to stable conditions. The step profiles in the topographic and damping contrast exhibit rapid jumps, as shown in Fig. 4(b). The adsorption of sample clusters possibly gives a charge to the apex in a stable manner. By zooming into the terrace, we obtain a clear atomic resolution with an atomic corrugation of about 4 Hz, as shown in Fig. 4(c). This atomic contrast corresponds to imaging the Ca sublattice as apparent when imaging with a negatively terminated tip.[19] The atomic contrast on the $CaF_2(111)$ surface appears to be most enhanced when imaging with this fluoride cluster tip when comparing results with those from the other tips. Apparently, the cluster exposes a negative ion at the tip end to the surface, enhancing the attractive interaction above Ca atoms.

V. CONCLUSIONS

In summary, we have prepared three types of tips with different materials at their apex and applied them to NC-AFM imaging of the (111) face of CaF_2 as a prototype ionic crystal. The as-supplied oxidized Si tip with clusters of the same material as that of the sample yields the strongest atomic contrast. This is attributed to the formation of a strong interaction between the polar tip and the sample at the atomic scale through ionic bonding forces. An oxidized Si tip without an attached cluster can carry charge, but this does not contribute to an enhancement of atomic contrast. Also, the silicon nanopillar and the carbon nanopillar tips do not show enhanced atomic contrast. To obtain a good quality in NC-AFM images with atomic resolution on an ionic material, one has to select a material that will provide a strong interaction between an ion stabilized at the tip apex and the ions on the sample. This is a polar tip that can most easily be prepared by picking up a cluster of the sample material. This underpins the general notion that such a surface is best imaged by a nanotip made of its own material.

[1]S. Orisaka, T. Minobe, T. Uchihashi, Y. Sugawara, and S. Morita, Appl. Surf. Sci. **140**, 243 (1999).

[2]T. König, G. H. Simon, H. P. Rust, and M. Heyde, Appl. Phys. Lett. **95**, 083116 (2009).

[3]H. Hölscher, W. Allers, U. D. Schwarz, A. Schwarz, and R. Wiesendanger, Phys. Rev. B **62**, 6967 (2000).

[4]B. J. Albers, T. C. Schwendemann, M. Z. Baykara, N. Pilet, M. Liebmann, E. I. Altman, and U. D. Schwarz, Nat. Nanotechnol. **4**, 307 (2009).

[5]S. Hembacher, F. J. Giessibl, J. Mannhart, and C. F. Quate, Proc. Natl. Acad. Sci. U.S.A. **100**, 12539 (2003).

[6]F. J. Giessibl, Appl. Phys. Lett. **76**, 1470 (2000).

[7]M. A. Lantz, H. J. Hug, R. Hoffmann, P. J. A. van Schendel, P. Kappenberger, S. Martin, A. Baratoff, and H. J. Güntherodt, Science **291**, 2580 (2001).

[8]T. Arai and M. Tomitori, Phys. Rev. Lett. **93**, 256101 (2004).

[9]Y. Sugimoto, P. Jelinek, P. Pou, M. Abe, S. Morita, R. Perez, and Ó. Custance, Phys. Rev. Lett. **98**, 106104 (2007).

[10]Y. Sugimoto, P. Pou, M. Abe, P. Jelinek, R. Pérez, S. Morita, and Ó. Custance, Nature (London) **446**, 64 (2007).

[11]C. Barth and M. Reichling, Nature (London) **414**, 54 (2001).

[12]S. Torbrügge, M. Reichling, A. Ishiyama, S. Morita, and Ó. Custance, Phys. Rev. Lett. **99**, 056101 (2007).

[13]S. Hirth, F. Ostendorf, and M. Reichling, Nanotechnology **17**, S148 (2006).

[14]S. Gritschneder, Y. Namai, Y. Iwasawa, and M. Reichling, Nanotechnology **16**, S41 (2005).

[15]M. Reichling and C. Barth, Phys. Rev. Lett. **83**, 768 (1999).

[16]A. V. Puchina, V. E. Puchin, M. Huisinga, R. Bennewitz, and M. Reichling, Surf. Sci. **402–404**, 687 (1998).

[17]C. Barth and M. Reichling, Surf. Sci. **470**, L99 (2000).

[18]V. E. Puchin, A. V. Puchina, M. Huisinga, and M. Reichling, J. Phys.: Condens. Matter **13**, 2081 (2001).

[19]A. S. Foster, C. Barth, A. L. Shluger, and M. Reichling, Phys. Rev. Lett. **86**, 2373 (2001).

[20]C. Barth, A. S. Foster, M. Reichling, and A. L. Shluger, J. Phys.: Condens. Matter **13**, 2061 (2001).

[21]T. Arai and M. Tomitori, Appl. Phys. A: Mater. Sci. Process. **66**, S319 (1998).

[22]M. Tomitori and T. Arai, Appl. Surf. Sci. **140**, 432 (1999).

[23]T. Arai and M. Tomitori, Appl. Phys. Lett. **86**, 073110 (2005).

[24]Z. A. Ansari, T. Arai, and M. Tomitori, Nanotechnology **18**, 084020 (2007).

[25]L. Gross, F. Mohn, N. Moll, P. Liljeroth, and G. Meyer, Science **325**, 1110 (2009).

[26]W. A. Hofer, A. S. Foster, and A. L. Shluger, Rev. Mod. Phys. **75**, 1287 (2003).

[27]P. Pou, S. A. Ghasemi, P. Jelinek, T. Lenosky, S. Goedecker, and R. Pérez, Nanotechnology **20**, 264015 (2009).

[28]J. V. Lauritsen *et al.*, Nanotechnology **17**, 3436 (2006).

[29]G. H. Enevoldsen, A. S. Foster, M. C. Christensen, J. V. Lauritsen, and F. Besenbacher, Phys. Rev. B **76**, 205415 (2007).

[30]G. H. Enevoldsen, H. P. Pinto, A. S. Foster, M. C. R. Jensen, A. Kühnle, M. Reichling, W. A. Hofer, J. V. Lauritsen, and F. Besenbacher, Phys. Rev. B **78**, 045416 (2008).

[31]R. Bechstein, C. González, J. Schütte, P. Jelínek, R. Pérez, and A. Kühnle, Nanotechnology **20**, 505703 (2009).

[32]H. H. Pieper, K. Venkataramani, S. Torbrügge, S. Bahr, J. V. Lauritsen, F. Besenbacher, A. Kühnle, and M. Reichling, Phys. Chem. Chem. Phys. **12**, 12436 (2010).

[33]A. S. Foster, C. Barth, A. L. Shluger, R. M. Nieminen, and M. Reichling, Phys. Rev. B **66**, 235417 (2002).

[34]A. S. Foster, A. Y. Gal, J. D. Gale, Y. J. Lee, R. M. Nieminen, and A. L. Shluger, Phys. Rev. Lett. **92**, 036101 (2004).

[35]A. S. Foster, A. L. Shluger, and R. M. Nieminen, Nanotechnology **15**, S60 (2004).

[36]M. Wendel, H. Lorenz, and J. P. Kotthaus, Appl. Phys. Lett. **67**, 3732 (1995).

[37]J. Lübbe, L. Tröger, S. Torbrügge, R. Bechstein, A. Kühnle, and M. Reichling, Meas. Sci. Technol. **21**, 125501 (2010).

[38]L. Tröger, J. Schütte, F. Ostendorf, A. Kühnle, and M. Reichling, Rev. Sci. Instrum. **80**, 063703 (2009).

[39]S. Gritschneder and M. Reichling, Nanotechnology **18**, 044024 (2007).

[40]S. Torbrügge, J. Lübbe, L. Tröger, M. Cranney, T. Eguchi, Y. Hasegawa, and M. Reichling, Rev. Sci. Instrum. **79**, 083701 (2008).

[41]T. Arai, S. Gritschneder, L. Tröger, and M. Reichling, Nanotechnology **15**, 1302 (2004).

[42]T. Arai (unpublished).